Supporting Information

Materials and Methods

Glucose and fatty acid uptake, lipogenesis, lipolysis and fatty acid oxidation. Glucose uptake was determined in isolated fat pads or skeletal muscle strips as described [1]. For measuring fatty acid uptake, epididymal adipose tissue or soleus muscle was incubated in preoxygenated buffer (120 mM NaCl, 4.8 mM KCl, 1.2 mM $MgSO_4$, 25 mM $NaHCO_3$, 1.2 mM NaH_2PO_4, 1.3 mM $CaCl_2$, pH7.4) for 30 minutes at 37°C. This was followed by another 30 minutes of incubation in fresh buffer with or without 100 nM insulin. Fatty acid uptake was initiated by adding 20 μM palmitic acid and 0.5 μCi/ml ^{3}H-palmitic acid. The reaction was stopped after five minutes. Non-specific uptake was measured in the presence of excess amount of palmitate (2 mM) and subtracted from all other values. The tissues were dissolved in 1M NaOH and neutralized with 1M HCl.

For assaying lipogenesis, adipose tissue was incubated in preoxygenated buffer containing 5.5 mM glucose in the presence of [U-^{14}C]glucose (1 μCi/ml) or ^3H_2O (1 μCi/ml). After two hours of incubation, total lipids were extracted from the tissues by chloroform/methanol method as described [1]. The radioactivity was determined by scintillation counting and results normalized against the total protein amount.

For lipolysis analysis, the epididymal fat pad was incubated in oxygenated Krebs-Ringer solution (120 mM NaCl, 4.8 mM KCl, 1.3 mM $CaCl_2$, 1.2 mM $MgSO_4$, 1.2 mM KH_2PO_4, 25 mM $NaHCO_3$, 6 mM glucose and 0.1 mM ascorbic acid, pH 7.6) at 37°C for 60 minutes in sealed plastic vials oscillating at 50 times/min. The amount of glycerol released into the media was measured with a colorimetric assay kit from Cayman Chemical Co. (Ann Arbor, MI, USA). The triglyceride contents were measured in adipose tissue and the results expressed in micromoles of released glycerol per mmol of tissue triglyceride in each reaction.

The rate of fatty acid oxidation was measured by the production of $^{14}CO_2$ from [1-^{14}C] palmitic acid using mitochondria fractions from adipose, liver and muscle tissues as described [2]. In brief, mitochondria were isolated from individual tissues as described [3] and mixed with reaction buffer (100 mM sucrose, 10 mM Tris-HCl, 5 mM KH_2PO_4, 0.2 mM EDTA, 0.3% BSA, 80 mM KCl, 1 mM $MgCl_2$, 2 mM L-carnitine, 0.1 mM malate, 0.05 mM coenzyme A, pH 8.0). After adding 2 mM ATP, 1 mM DTT, 0.5 mM palmitic acid and 0.4 μCi/ml [1-^{14}C] palmitic acid, the reaction was continued at 37°C for 60 minutes and then stopped with 1 M perchloric acid. The released ^{14}CO2 was captured by filter paper rinsed with concentrated hyamine hydroxide. The filter paper was transferred to scintillation vial for radioactivity counting.

ACC activity. ACC activity was measured as described [4] with modifications. Briefly, tissue was homogenized on ice in buffer containing 50 mM Tris-HCl (pH 7.4), 250 mM mannitol, 1 mM EDTA, 1 mM DTT, 50 mM NaCl, 50 mM NaF, 1 mM PMSF, 5 mM $Na_2H_2O_7$ and protease inhibitor cocktail. After centrifugation at 14,000 *g* for 30 minutes at 4°C, the supernatant was used as a crude enzyme fraction. The protein concentration was determined by BCA assay (Thermo Scientific, Rockford, IL, USA). For ACC assay, the crude enzyme fraction with equal amount of proteins was incubated with reaction mixture containing 100 mM Tris-HCl (pH 7.5), 1 mM DTT, 2.1 mM ATP, 125 μM acetyl-CoA, 6 mM $MgCl_2$, 100 mM KCl, 10 mM sodium citrate, 1mg/ml BSA, 18 mM NaH[^{14}C]O_3 (0.5 mCi/mmol) for 30 minutes at 37°C. The reaction was stopped by the addition of 1 M $HClO_4$. After centrifugation at 2000 *g* for 15 minutes, the supernatant was transferred into a vial and dried. The sample was resolved in a scintillation cocktail and the bound [^{14}C]bicarbonate was quantified by a liquid scintillation counter. ACC activity was expressed in units: 1 unit = 1 nmol fixed HCO_3^-/min/mg protein.

ELISA quantification of total biotin. Free biotin and biotinylated proteins in serum and tissue samples were measured using commercially available ELISA kit (Immundiagnosti, Bensheim, Germany) according to manufacturer's instructions. In brief, equal amounts of serum and tissues samples were mixed with HRP-conjugated avidin and incubated for two hours at room temperature. The mixture was then transferred to wells of biotinyl-BSA-coated plate and incubated for another four hours at room temperature. After adding the substrate, the absorbance at 450 nm was measured. The detection range of biotin was 0.15–500 nM.

Synthesis of biotinyl-5'-AMP. Adenylic acid (35 mg, 0.1 mmol, 1 eq.) and d-biotin (25 mg, 0.1 mmol, 1 eq.) were dissolved in 75% aqueous pyridine (0.5 ml) at 0°C. To the solution, DCC (413 mg, 2.0 mmol, 20 eq.) in pyridine (0.5 ml) precooled to 0 °C was added slowly. The mixture was stirred at 0°C for 24 hr. DCC was removed by filtering through a pad of celite. The crude product was purified by preparative HPLC (Gradient: 5-20% CH_3CN/H_2O over 30 min, 20-65% CH_3CN/H_2O over 10 min at a flow rate of 10 ml/min), followed by concentration and lyophilization. The identity and purity of biotinyl-5'-AMP was confirmed by mass spectrometry analysis.

Preparation of stromal vascular cell fraction (SVF) and mature adipocytes. Adipose tissue was digested with collagenase (1 mg/ml) for 30 min at 37°C with shaking. The cell suspensions were filtered through a 40 μm Cell Strainer (BD Biosciences, San Jose, CA, USA) and centrifuged at 500 g for 10 min. The supernatant containing the mature adipocytes was collected. The SVF pellet was washed with lysis buffer (155 mM NH_4Cl, 10 mM $KHCO_3$, and 0.1 mM Na_2EDTA, pH 7.4) to remove red blood cells. The adipocyte fraction and SVF pellets were subsequently used for Western blotting.

Measurement of tissue NAD^+/NADH contents. EnzyChrom™ NAD^+/NADH assay kits (BioAssay Systems, Hayward, CA, USA) were used. In brief, tissues (20 mg) were homogenized in extraction buffers and the total amount of NAD^+/NADH was measured

according to the instructions from manufacturer. The results were calculated as the amount of NAD^+ or NADH (nmol) per mg of tissue weight.

Quantitative RT-PCR analysis. Total RNA were isolated from adipose tissue using TRIZOL Reagent (Invitrogen, Carlsbad, CA) and reverse transcribed using Superscript III reverse transcription system (Invitrogen). Oligonucleotide primers were designed using GenScript Online Tools (http://www.genscript.com/ssl-bin/app/primer). Primer sequences are listed in Supplementary Table S2. Quantitation of target gene mRNA was performed in 96 well plates using QuantiTect® SYBR®Green PCR Master Mix (Qiagen, Hilden, Germany) and an ABI PRISM 7900 HT Sequence Detection System (Applied Biosystems, Foster city, CA). Quantification was achieved using Ct values that were normalized with beta-actin as a reference control.

Western blotting and co-immunoprecipitation. Antibodies against ACC, acetylated lysine and DYKDDDDK Flag-tag were purchased from Cell Signaling (Beverly, MA, USA). Antibodies against SIRT1 and acetylated histone H4 (K5, K8, K12 and K16) were from Millipore (Billerica, MA, USA). Monoclonal antibody against beta-actin and streptavidin HRP conjugate were purchased from Sigma. For Western Blotting, proteins derived from cell or tissue lysates were separated by SDS-PAGE and transferred to polyvinylidene difluoride membranes. Following blocking, membranes were probed with various primary antibodies to determine different levels of protein expressions. Streptavidin HRP conjugate was used for probing biotinylated proteins. Immunoreactive antibody-antigen complexes were visualized with the enhanced chemiluminescence reagents from GE Healthcare (Uppsala, Sweden).

For co-immunoprecipitation, tissues or cells were solubilized in radioimmunoprecipitation assay lysis buffer. Same amounts of protein lysates (500 μg) were incubated with specific antibody at 4°C overnight on a shaking platform. After washing

extensively with ice-cold PBS, the immunocomplexes were eluted with 0.1 mol/L glycine HCl (pH 3.0) and neutralized for SDS-PAGE and Western blotting.

Cloning and mutagenesis. The BCCP cDNA fragment of human ACC (3420-4457 nt, NM 198839.1) was cloned from HepG2 cells with the primers listed in Supplementary Table S1. After another two rounds of PCR to introduce sequences encoding a myc (EQKLISEEDL) and a Flag (DYKDDDDK) tag at 5' and 3' end, respectively, a NotI/XhoI fragment was subcloned into pcDNA 3.1 (+) vector to produce the mammalian expression vector pcDNA-BCCP.

Molecular docking The ICM-Pro 3.7-2b program [Molsoft] was applied to evaluate the binding of biotin or its metabolites to Sir2 [5]. Hydrogen and missing heavy atoms were added to the structure followed by local minimization using the conjugate gradient algorithm and analytical derivatives in the internal coordinate space. The energetically most favorable tautomeric state of His was chosen. Position of Asn and Gln were optimized to maximize hydrogen bonding. The correct stereochemistry and formal charges were assigned. Biotin was then assigned the MMFF atom types and charges, and subjected to a global energy optimization using the ICM stochastic optimization algorithm. A modified ECEPP/3 force-field with distance-dependent dielectric constant was used for energy calculations as implemented in ICM. The biased probability Monte Carlo minimization method consisted of the following steps: (1) a random conformation change of the free variables according to a predefined continuous probability distribution; (2) local energy minimization of analytical differentiable terms; (3) calculation of the complete energy including non-differentiable terms such as entropy and solvation energy; and (4) acceptance or rejection of the total energy based on the Metropolis criterion and return to step 1. The binding score was evaluated by binding energy, composes of grid energy, continuum electrostatic and entropy terms.

References

[1] Law IK, Xu A, Lam KS, Berger T, Mak TW, Vanhoutte PM, Liu JT, Sweeney G, Zhou M, Yang B and Wang Y. Lipocalin-2 deficiency attenuates insulin resistance associated with aging and obesity. Diabetes 2010; 59: 872-882.

[2] Hirschey MD, Shimazu T, Goetzman E, Jing E, Schwer B, Lombard DB, Grueter CA, Harris C, Biddinger S, Ilkayeva OR, Stevens RD, Li Y, Saha AK, Ruderman NB, Bain JR, Newgard CB, Farese RV, Jr., Alt FW, Kahn CR and Verdin E. SIRT3 regulates mitochondrial fatty-acid oxidation by reversible enzyme deacetylation. Nature 2010; 464: 121-125.

[3] Zhou M, Xu A, Tam PK, Lam KS, Chan L, Hoo RL, Liu J, Chow KH and Wang Y. Mitochondrial dysfunction contributes to the increased vulnerabilities of adiponectin knockout mice to liver injury. Hepatology 2008; 48: 1087-1096.

[4] Witters LA, Watts TD, Daniels DL and Evans JL. Insulin stimulates the dephosphorylation and activation of acetyl-CoA carboxylase. Proc Natl Acad Sci U S A 1988; 85: 5473-5477.

[5] Chow KH, Sun RW, Lam JB, Li CK, Xu A, Ma DL, Abagyan R, Wang Y and Che CM. A gold(III) porphyrin complex with antitumor properties targets the Wnt/beta-catenin pathway. Cancer Res 2010; 70: 329-337.

Table S1. List of primers used for cDNA cloning, site-directed mutagenesis and genotyping.

Experiment	Primer sequences
Subcloning hSIRT1	Forward: CTTATCGATATCTCGTCGTGCATCTTTTG
	Reveres: GGTATCGATGGCTACTTGTCATCGTCGTCCTTGTAGTCTGATTTGTTTGATGGATAGTT
Mutagenesis for hSIRT1(H363Y)	Forward: TAATT CAGTGTTATG GTTCCTTTGC
	Reverse: GCAAAGGAAC CATAACACTG AATTA
Genotyping I	Forward: TGGCCCCCATTGGTCACTCCT
(product 483 bp)	Reverse: GCCCGGCCCATTGTCTCCTT
Genotyping II	Forward: GCAAAGGAGCAGATTAGTAGGCGGC
(product 405 bp)	Reverse: CGAGGTCGACGGTATCGATGGCT
Genotyping III	Forward: TGCTCGCCTTGCTGTAGACTTCC
(PCR-RFLP)	Reverse: AAGCGGTTCATCAGCTGGGCA
	A PCR product 373 bp is digested with *NlaIII* to generate two fragments of 122 bp and 251 bp in AWSM samples.
Genotyping IV	Forward: TCCTGGACAATTCCAGCCATCTCT
(PCR-RFLP)	Reverse: AGATGCTGTTGCAAAGGAACCAT
	A PCR product 160 bp is digested with *NlaIII* to generate two fragments of 140 bp and 20 bp in AWSM samples.
Subcloning BCCP	Forward_1: GGGCTGAGTGACGGTGGACTGC
	Reverse_1: AGGGTCCCGGCCACACAACT
	Forward_2: ACCATGGAACAGAAACTGATTAGCGAAGAAGATCTGGGGCTGAGTGACGGTGGACTGC
	Reverse_2: CTACTTGTCATCGTCGTCCTTGTAGTCAGGGTCCCGGCCACACAACT
	Forward_3: AGCACAGTGGCGGCCGCACCATGGAACAGAAACTGATTAG
	Reverse_3: GCCCTCTAGACTCGAGCTACTTGTCATCGTCGTCCTT

Table S2. List of primers used for quantitative PCR analysis.

Gene name	Gene symbol	Accession ID	Sequence range	Product size (bp)	Primer sequences
Beta-actin	*Actb*	gi|145966868	930-1107	178	Forward 5'-AGTGTGACGTTGACATCCGT-3' Reverse 5'-CCACCGATCCACACAGAGTA-3'
Adipose triglyceride lipase (ATGL)	*Pnpla2*	gi|254826779	724-868	145	Forward 5'-AACACCAGCATCCAGTTCAA -3' Reverse 5'-GGTTCAGTAGGCCATTCCTC -3'
Holocarboxylase (HCS)	*Hlcs*	gi|146149144	1719-1881	163	Forward 5'-TGTGCTCTTTCCACTCTGCT-3' Reverse 5'-AAATATCGTTGGGCCACTTC-3'
Biotinidase	*Btd*	gi|270341335	325-469	145	Forward 5'-CAGCCCAGAAGGGTGTGCAGAT-3' Reverse 5'-CGAAAGGGCTCCAGACACGGG-3'
Acetyl-Coenzyme A carboxylase alpha (ACCα)	*Acaca*	gi|125656172	178-339	162	Forward 5'-CCTCCGTCAGCTCAGATACA -3' Reverse 5'-CTGGAGAAGCCACAGTGAAA -3'
Acetyl-Coenzyme A carboxylase beta (ACCβ)	*Acacb*	gi|157042797	3696-3892	197	Forward 5'-GGTGGAGTCCATCTTCCTGT -3' Reverse 5'-TGTTTAGCTCGTAGGCGATG -3'
Sodium-dependent vitamin transporter (SVMT)	*Slc5a6*	gi|294979173	1975-2129	155	Forward 5'-CCTTGGACTGTTCTTCCCAT-3' Reverse 5'-GGAAGGAGCTGGATCCATTA-3'
Adiponectin	*Adipoq*	gi|87252710	24-293	200	Forward 5'-ACGACACCAAAAGGGCTCAGGA-3' Reverse 5'-CCATCACGGCCTGGTGTGCC-3' '
Glucokinase	*Gck*	gi|118129970	48-247	200	Forward 5'-AGA GCA GAT CCT GGC AGA GT -3' Reverse 5'-TGG TTC CTC CCA GGT CTA AG -3'

Supplementary Figure 1

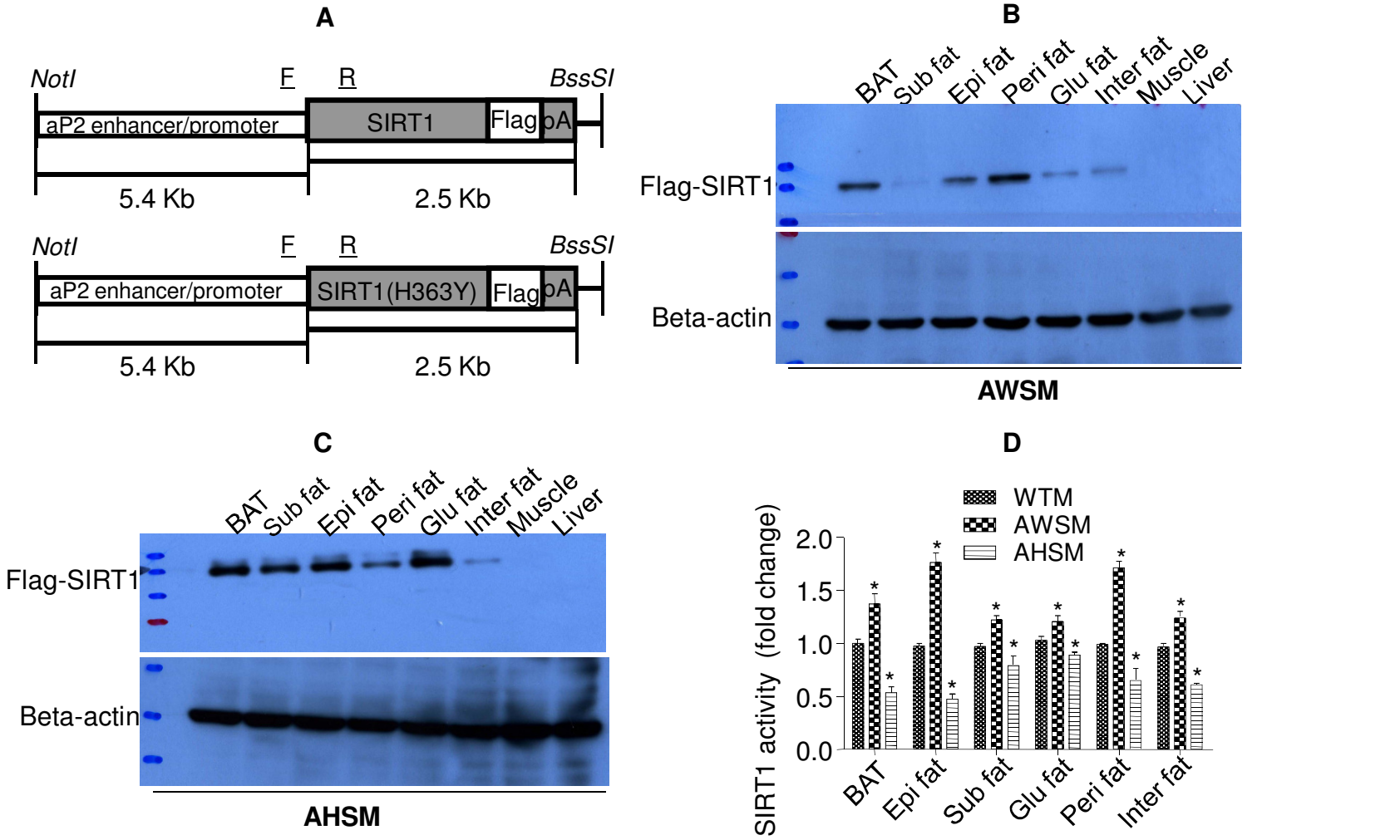

Supplementary Figure 1. **Establishment of transgenic mice selectively over-expressing human SIRT1 (hSIRT1) or its mutant hSIRT1(H363Y) in adipose tissues. (A)** Fragments of transgenic vectors for overexpressing Flag-tagged hSIRT1 (NM_012238.4) or hSIRT1(H363Y) under the control of an aP2 enhancer/promoter. **(B)** Representative image of Western blotting analysis of Flag-tagged hSIRT1 expression in tissues collected from AWSM. Beta-actin was probed as loading control. **(C)** Representative image of Western blotting analysis of Flag-tagged hSIRT1(H363Y) expression in tissues collected from AHSM. Beta-actin was probed as loading control. **(D)** Adipose SIRT1 activity was measured using commercial assay kits . The results are expressed as fold changes *versus* that of WTM control samples. *, $P < 0.05$ compared with WTM control group (n=3). Epi, epididymal fat; Glu, gluteal fat; Inter, interscapular fat; Peri, perirenal fat; Sub, subcutaneous fat; BAT, brown fat.

Supplementary Figure 2

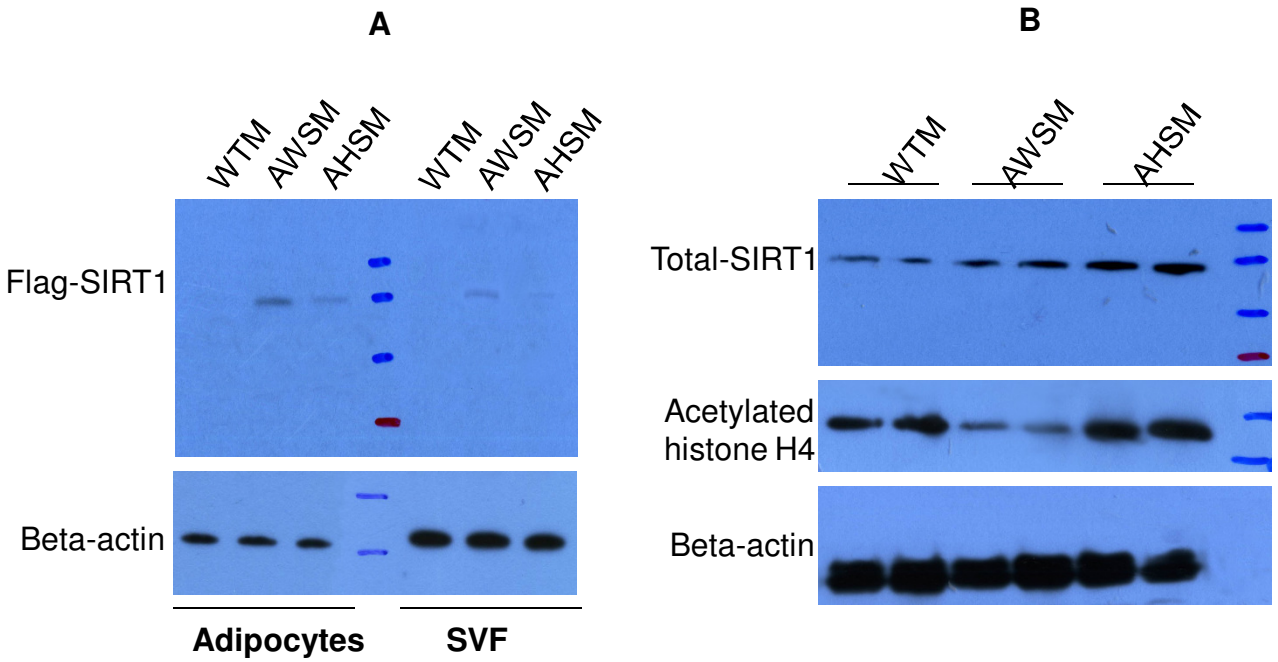

Supplementary Figure 2. Flag-tagged hSIRT1 and hSIRT1(H363Y) could be detected in adipocytes and stromal vascular fractions (SVF) isolated from the fat pads of transgenic animals. (A) Epididymal fat was isolated from WTM, AWSM and AHSM. After digesting with collagenase, adipocytes and SVF pellets were collected as described in Methods. Proteins (50 μg and 80 μg for adipocytes and SVF, respectively) were separated by SDS-PAGE and subjected to Western blotting using antibodies against the Flag-tag (top) and beta actin (bottom). **(B)** Increased expression of SIRT1 protein in adipose tissues of AWSM and AHSM was confirmed by Western blotting using an antibody recognizing both murine and human SIRT1 (top). The amount of acetylated histone H4 (K5, K8, K12, K16) was probed with specific antibody (middle). Beta actin was probed as the loading control (bottom).

Supplementary Figure 3

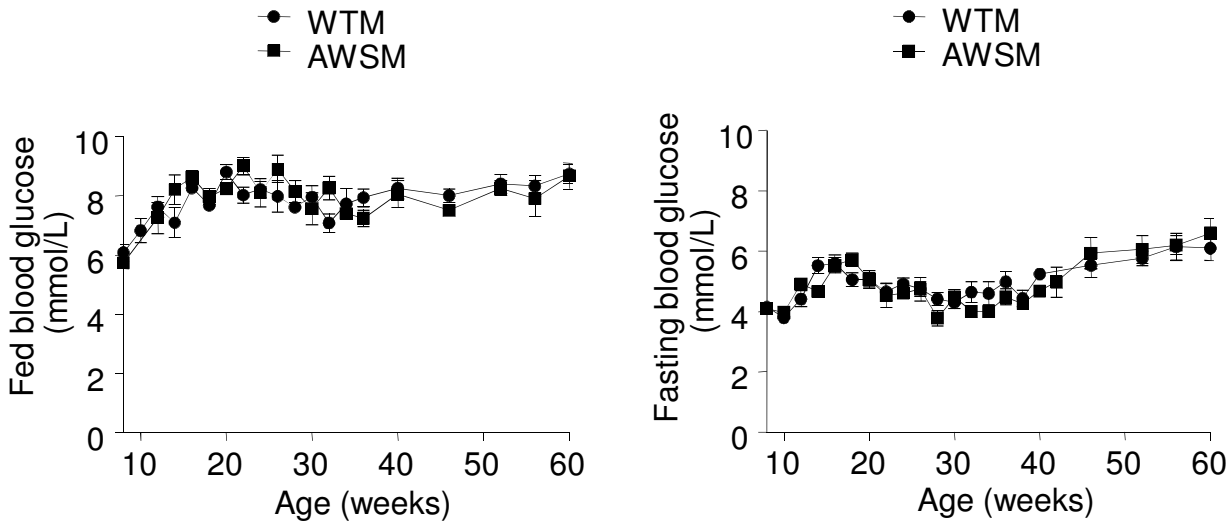

Supplementary Figure 3. Blood glucose levels were not different between WTM and AWSM. Fed blood glucose (left) was measured at 10am in mice fed *ad libitum*. Fasting blood glucose (right) was measured at 10am in mice that were starved for16 hours.

Supplementary Figure 4

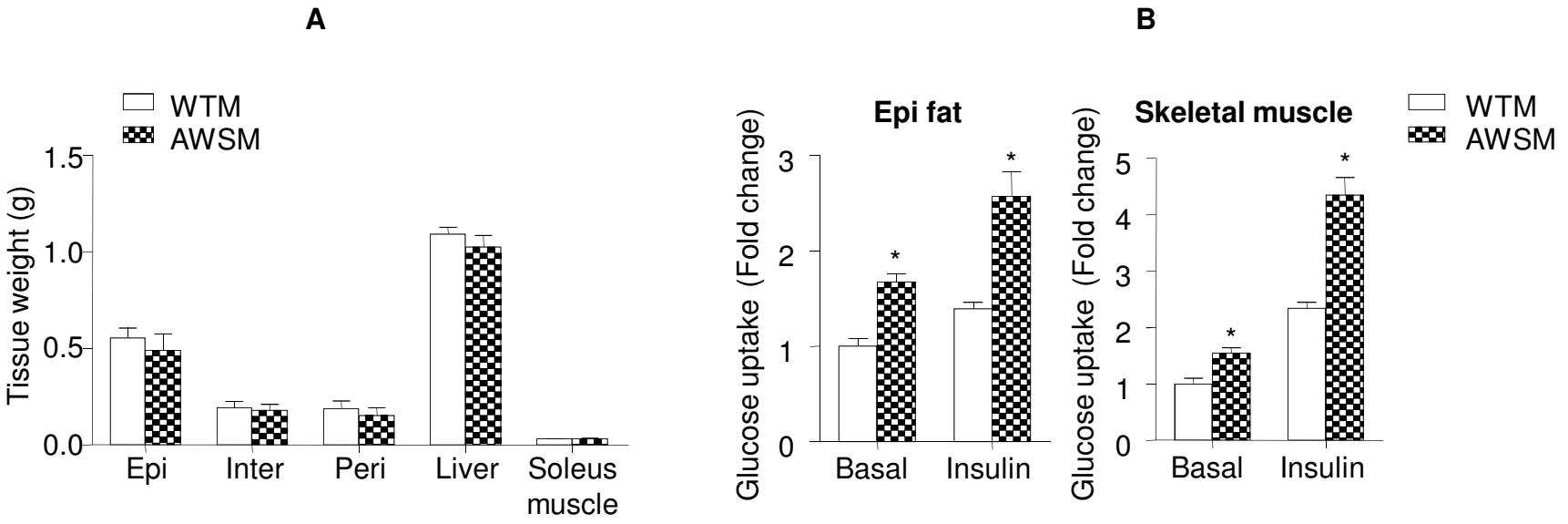

Supplementary Figure 4. Overexpression of hSIRT1 selectively in adipose tissue enhanced peripheral insulin sensitivity. (A) Tissue weights were recorded for WTM and AWSM sacrificed at the age of 36-week old. **(B)** Basal and insulin-stimulated glucose uptake was evaluated in epididymal (epi) adipose tissue and soleus muscle strips using [^{3}H]-2-deoxyglucuse as a tracer. The results are presented as fold changes against the basal glucose uptake of WTM control group. *, P<0.05 compared with WTM group (n=10).

Supplementary Figure 5

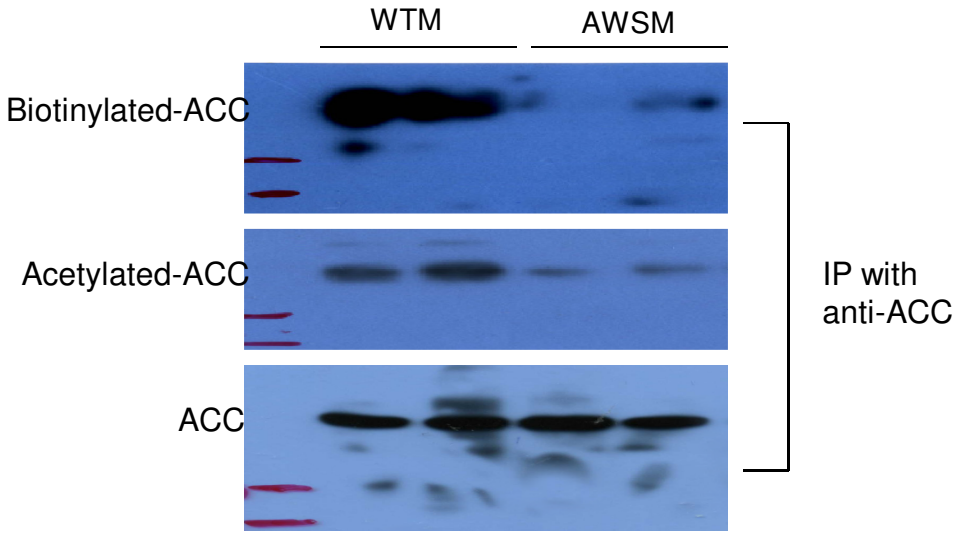

Supplementary Figure 5. **Decreased biotinylation and acetylation of ACC in adipose tissues of AWSM.** Immunoprecipitation (IP) was performed using specific antibody against ACC. The biotinylation and acetylation levels of the precipitated ACC protein were probed by Western blotting.

Supplementary Figure 6

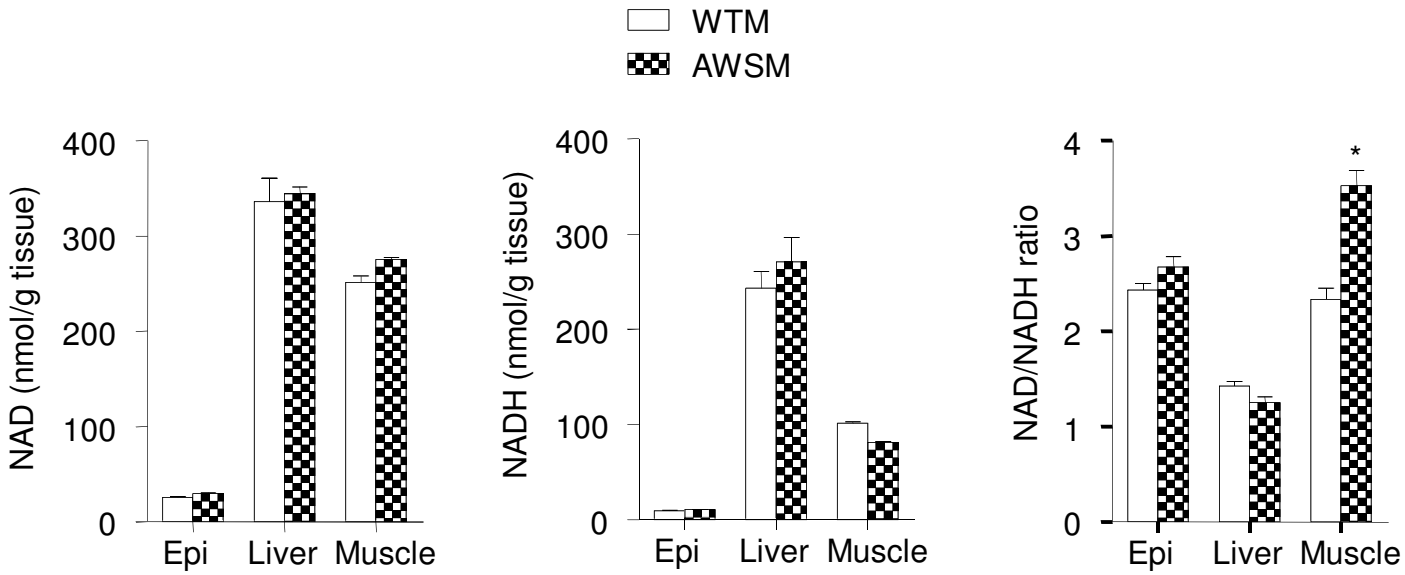

Supplementary Figure 6. **Skeletal muscle of AWSM showed significantly increased NAD/NADH ratio.** The amount of NAD and NADH was measured in epi fat, liver and skeletal muscle of WTM and AWSM mice (36-weeks old). The ratio of NAD/NADH was calculated and presented in the right panel. *, $P<0.05$ compared with WTM control group (n=5).

Supplementary Figure 7

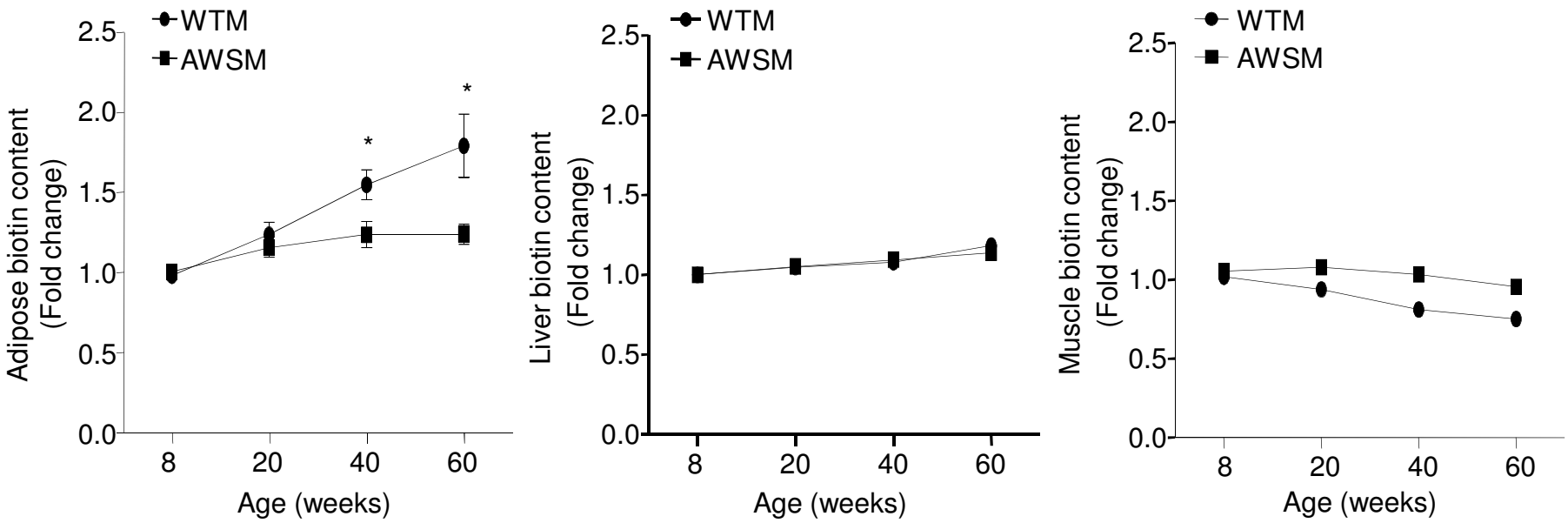

Supplementary Figure 7. **Ageing-dependent biotin accumulation in adipose tissue was alleviated in AWSM.** Tissue extracts from epididymal fat, liver and skeletal muscle of WTM and AWSM were used for measuring total biotin content using the commercially available ELISA kits as described in Methods. The results are presented as fold change against the values of 8-weeks old mice. *, $P<0.05$ compared with WTM control group (n=3-6).

Supplementary Figure 8

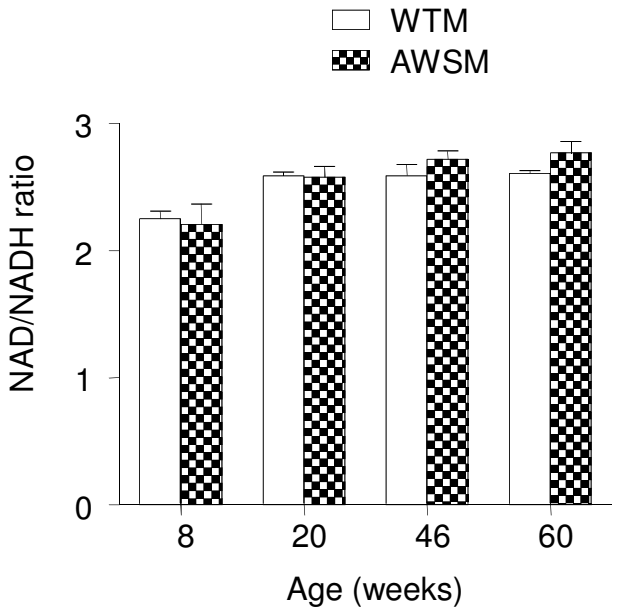

Supplementary Figure 8. **The NAD/NADH ratio in adipose tissues of WTM and AWSM was similar.** The amount of NAD and NADH was measured in epididymal fat collected from WTM and AWSM at different ages. The ratio of NAD/NADH was calculated and presented. (n=5)

Supplementary Figure 9

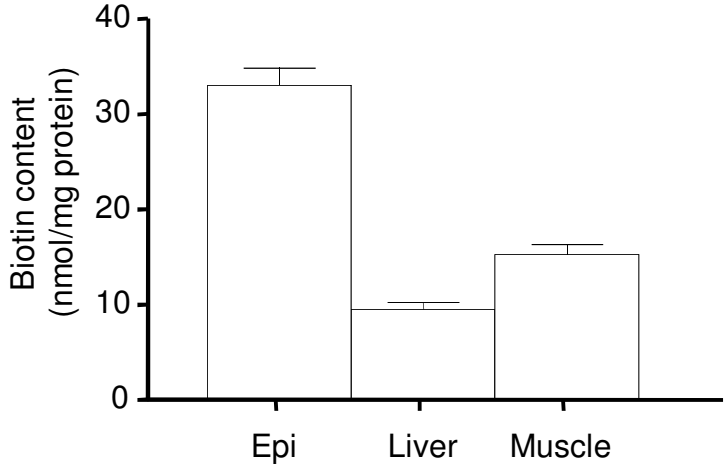

Supplementary Figure 9. **Biotin contents in epididymal tissue (epi), liver and skeletal muscle of wild type C57BL/6J mice.** The amount of biotin was measured using commercial kit and results calculated against protein content. (n=5)

Supplementary Figure 10

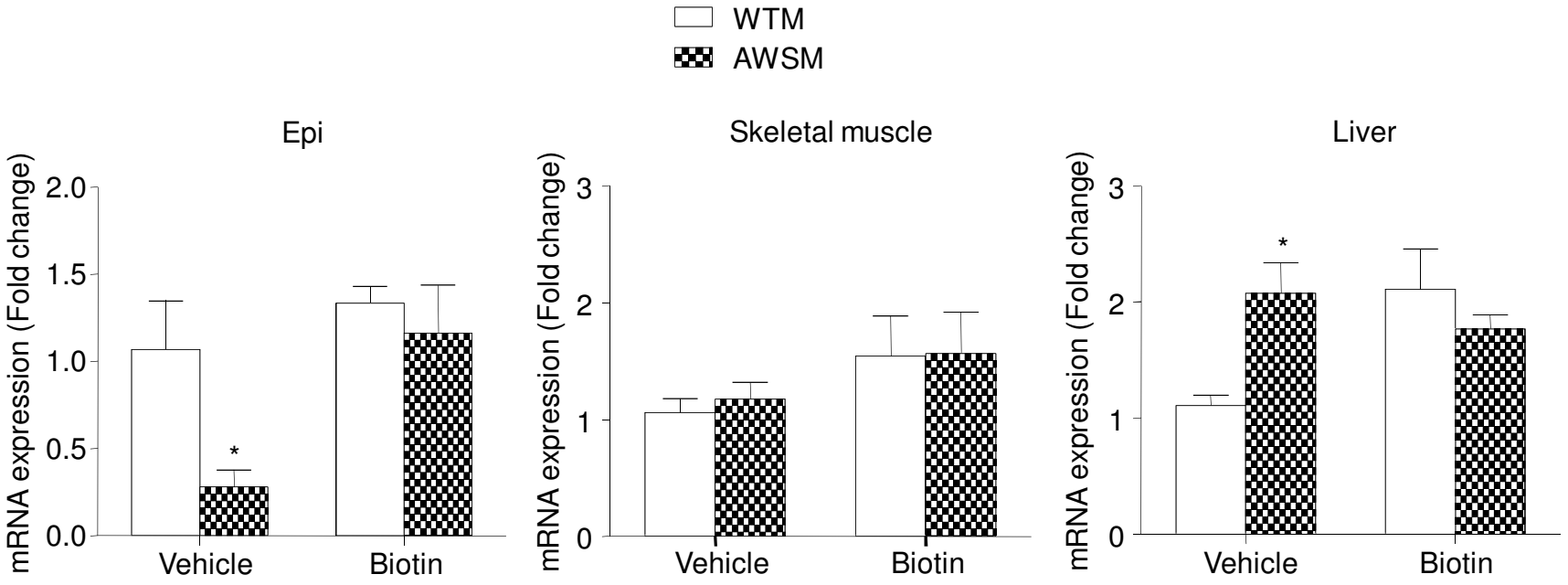

Supplementary Figure 10. **Chronic supplementation of biotin abolished the differences of glucokinase gene expression between WTM and AWSM mice.** Epididymal adipose (epi), skeletal muscle and liver tissues were collected from vehicle- or biotin-treated WTM and AWSM mice for quantitative PCR analysis of glucokinase mRNA levels. *, $P<0.05$ compared with corresponding WTM control group (n=3-5).

Supplementary Figure 11

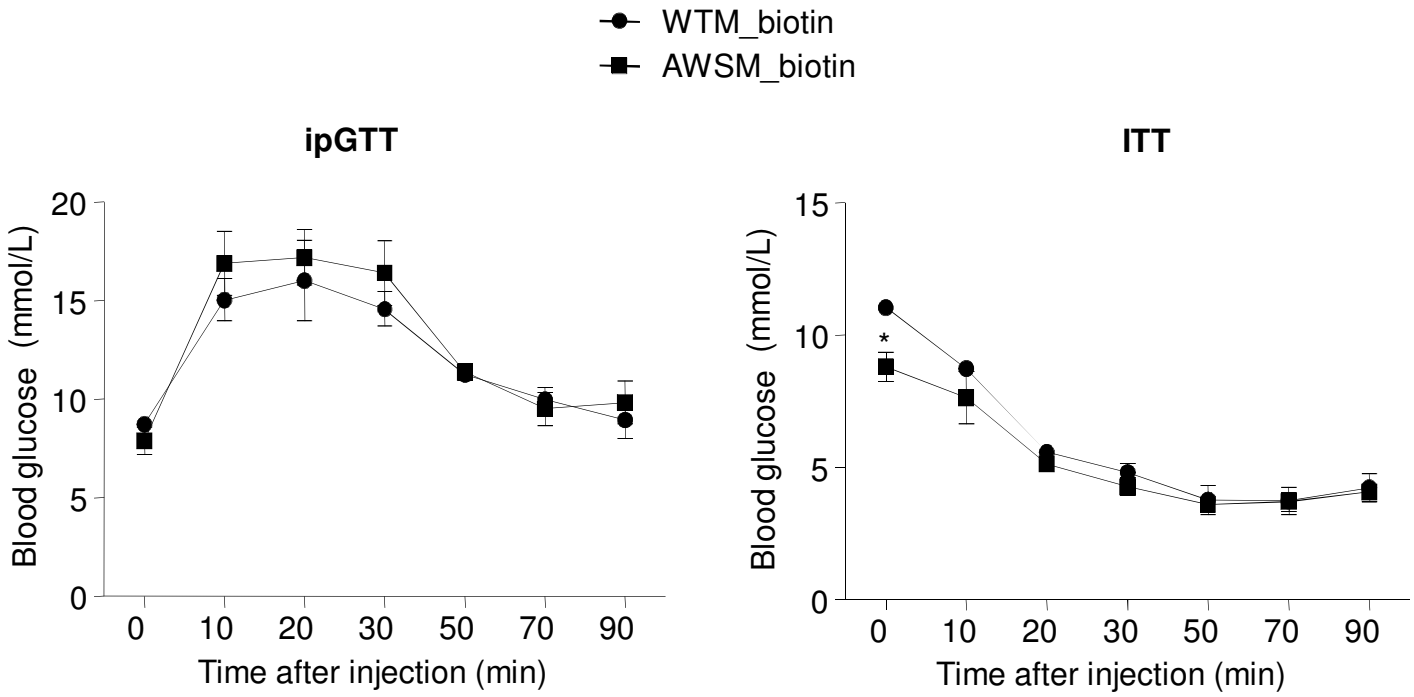

Supplementary Figure 11. **Chronic supplementation of biotin abolished the beneficial metabolic effects of adipose SIRT1 in AWSM.** Intraperitoneal glucose tolerance tests (ipGTT) and insulin tolerance tests (ITT) were performed for WTM and AWSM (60-weeks old) subjected to biotin treatment. Biotin-treated WTM showed significantly higher blood glucose levels after six hours of fasting. *, $P<0.05$ compared with biotin-treated WTM group (n=10).

Supplementary Figure 12

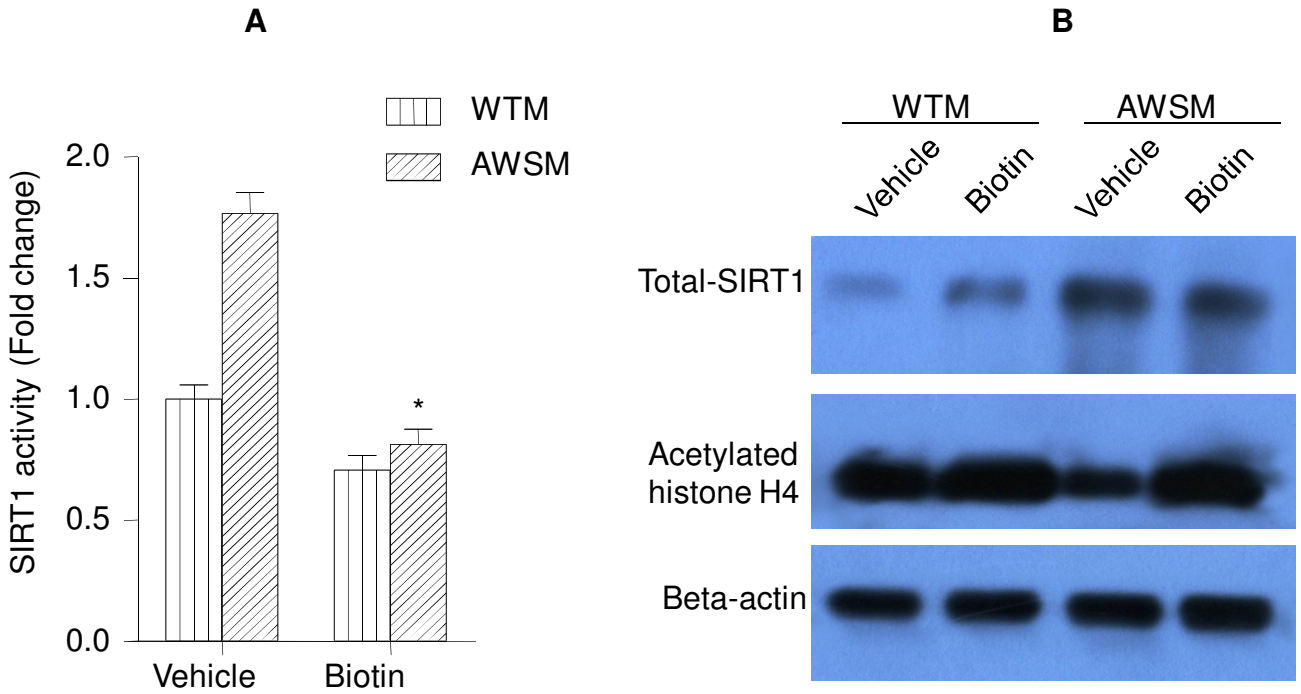

Supplementary Figure 12. **Biotin supplementation reduced adipose SIRT1 activity.** Epididymal fat was isolated from WTM and AWSM treated with vehicle or biotin. **(A)** SIRT1 activity was measured in tissue lysates using commercial assay kits as described in Methods. **(B)** Proteins (100 μg) were separated by SDS-PAGE and subjected to Western blotting using antibodies against SIRT1 (human and murine) and acetylated histone H4 (K5, K8, K12, K16). Beta actin was probed as loading control. *, $P<0.01$ compared with vehicle-treated AWSM (n=6)

Supplementary Figure 13

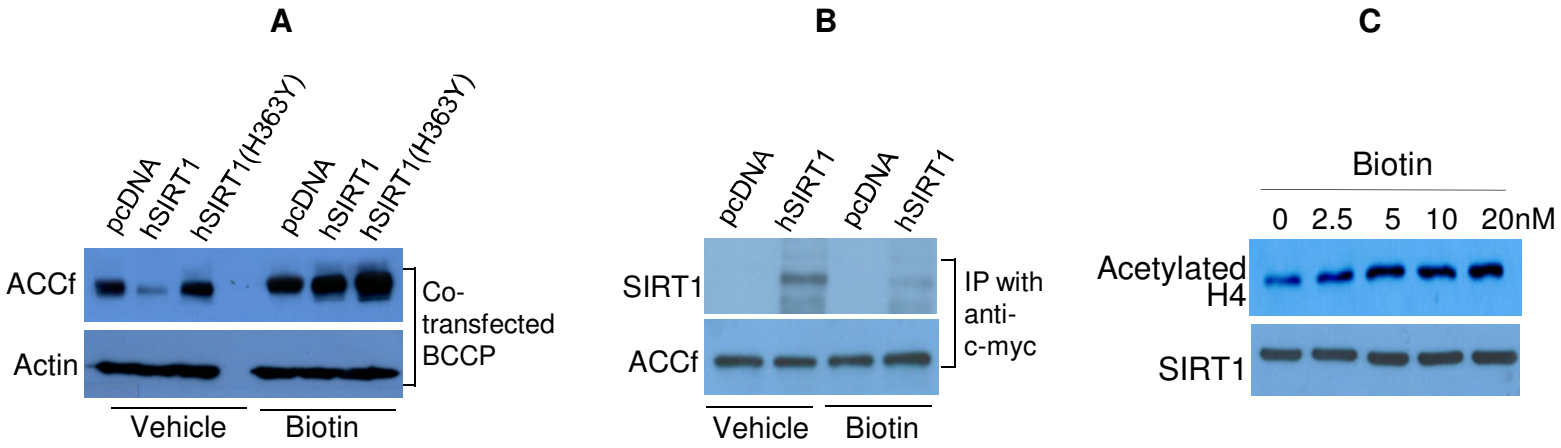

Supplementary Figure 13. Biotin inhibited SIRT1-mediated regulation of ACC protein expression. **(A)** The protein abundance of ACCf was evaluated in 3T3-L1 cells co-transfected pcDNA-BCCP, together with pcDNA, pcDNA-hSIRT1 or pcDNA-hSIRT1(H363Y). Cells were treated with vehicle or biotin (10 nM). Anti-Flag antibody was used for detecting ACCf by Western blotting. **(B)** Immunoprecipitation was performed in 3T3-L1 cells overexpressing hSIRT1 and/or ACCf, using antibodies against c-myc tag. The presence of SIRT1 in the immuno-complex was probed with specific antibodies recognizing both murine and human SIRT1. **(C)** Acetylated histone H4 was detected by Western blotting in 3T3-L1 adipocytes treated with increasing concentrations of biotin.

Supplementary Figure 14

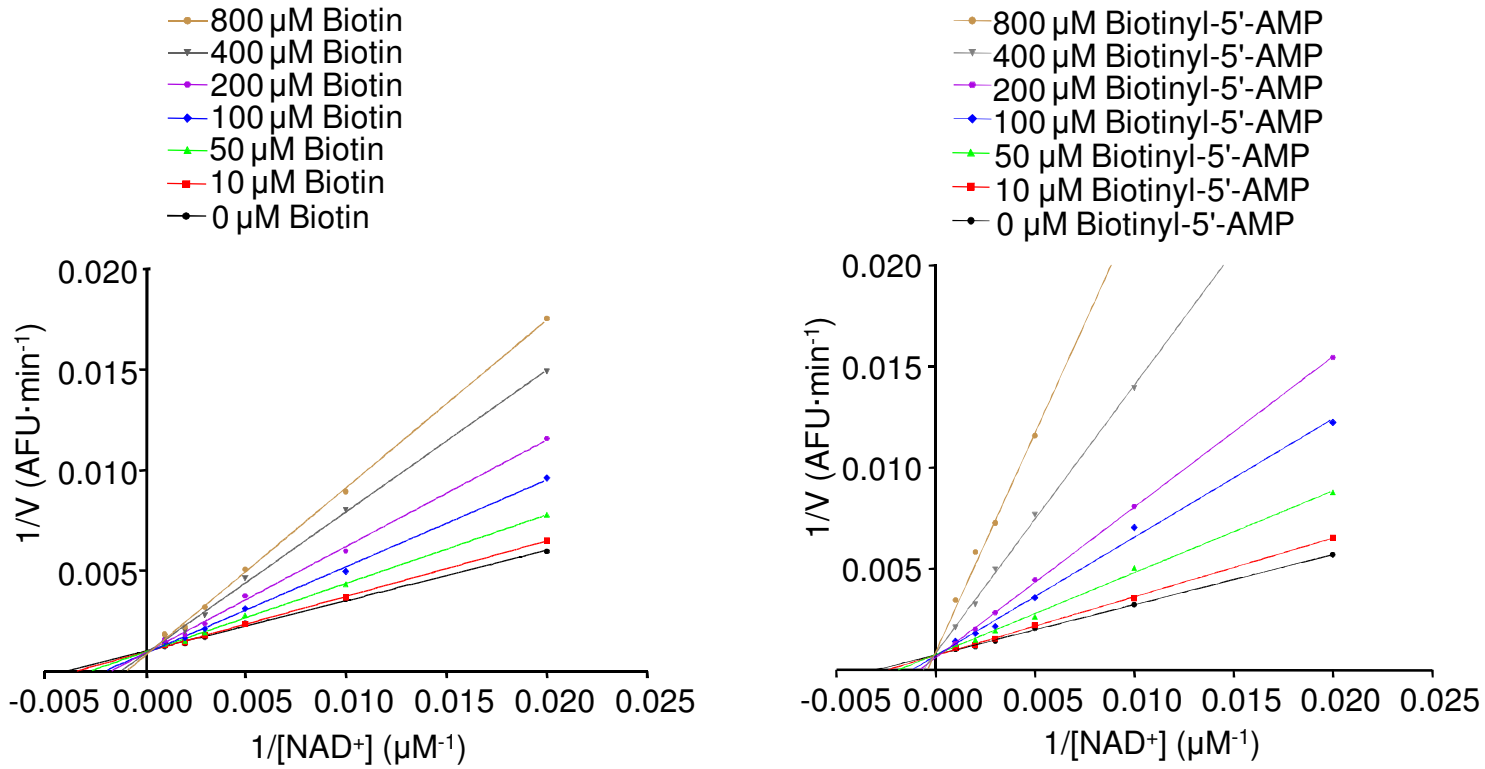

Supplementary Figure 14. Biotin and biotinyl-5'-AMP acted as competitive inhibitors of SIRT1. Left: SIRT1 activity was measured in the presence of different concentrations of NAD^+ and/or biotin. **Right:** SIRT1 activity was measured in the presence of different concentrations of NAD^+ and/or biotinyl-5'-AMP. Data are shown as Lineweaver-Burk double-reciprocal plots of arbitrary fluorescence units (AFU) min^{-1} *versus* $1/[NAD^+]$ (μM^{-1}).

Supplementary Figure 15

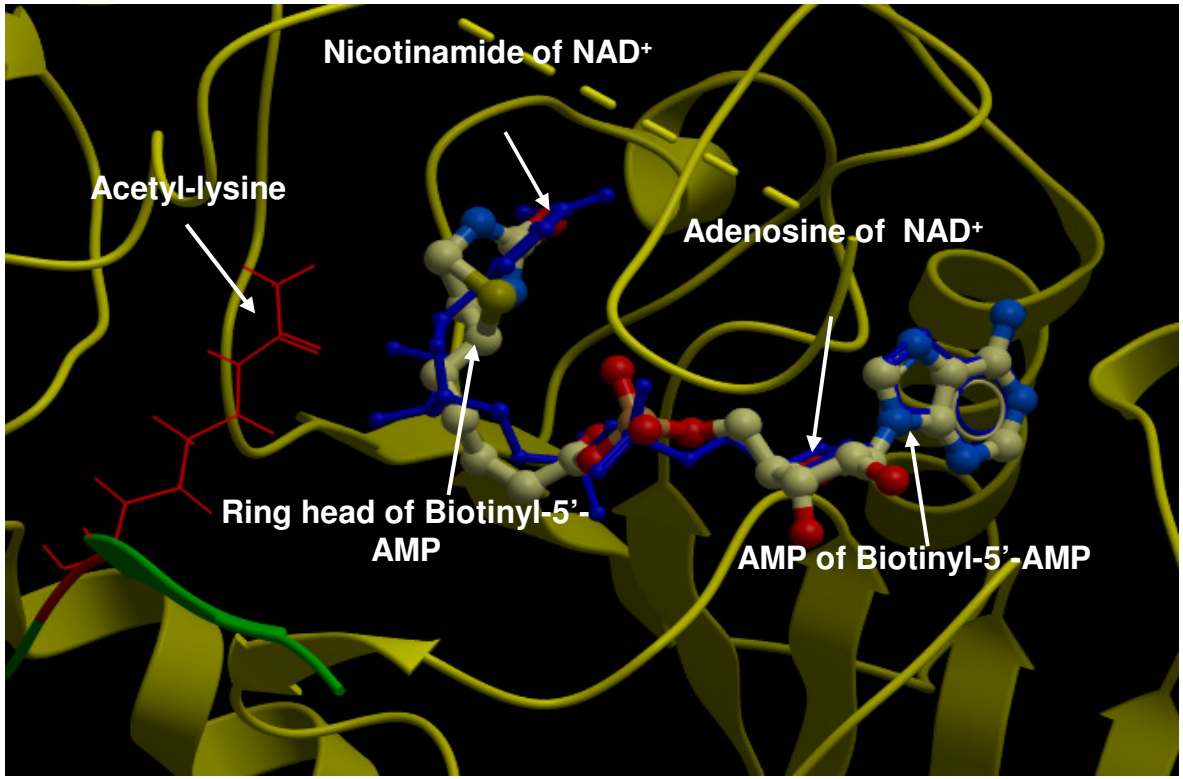

Supplementary Figure 15. Docking model (lowest-energy) for the binding of biotinyl-5'-AMP with Sir2 homologue (ribbon form, yellow). Biotinyl-5'-AMP (thick ball and stick format, blue for N, red for O, and white for C) occupies the binding pocket of NAD^+ (thin ball and stick format, blue). Green ribbon represents the p53 peptide (the acetyl-lysine residue is shown in red wire format).

Supplementary Figure 16

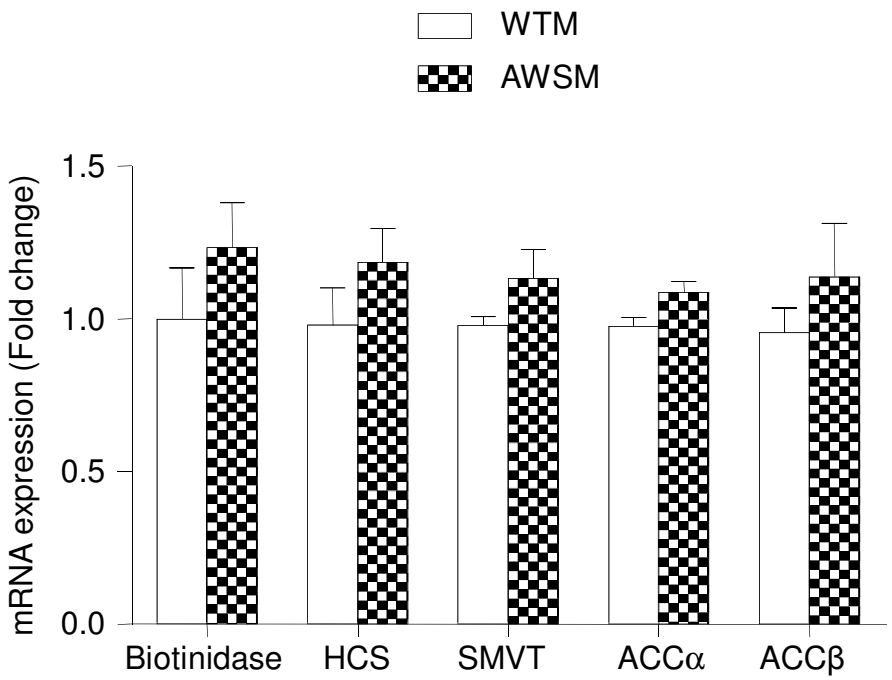

Supplementary Figure 16. The mRNA expression levels of biotinidase, holocarboxylase synthetase (HCS), sodium-dependent multivitamin transporter (SMVT), acetyl CoA carboxylase alpha (ACCα) and ACCβ in adipose tissues of AWSM were not significantly different from those of WTM. RNA was extracted from epididymal fat of WTM and AWSM. Quantitative PCR was performed for comparing the mRNA expression levels of the above genes. (n=5)